ACS OMEGA

http://pubs.acs.org/journal/acsodf

Article

Toward the Development of GE11-Based Radioligands for Imaging of Epidermal Growth Factor Receptor-Positive Tumors

Benedikt Judmann,[⊥] Diana Braun,[⊥] Ralf Schirrmacher, Björn Wängler, Gert Fricker, and Carmen Wängler*

Cite This: *ACS Omega* 2022, 7, 27690−27702

Read Online

ACCESS | Metrics & More | Article Recommendations | Supporting Information

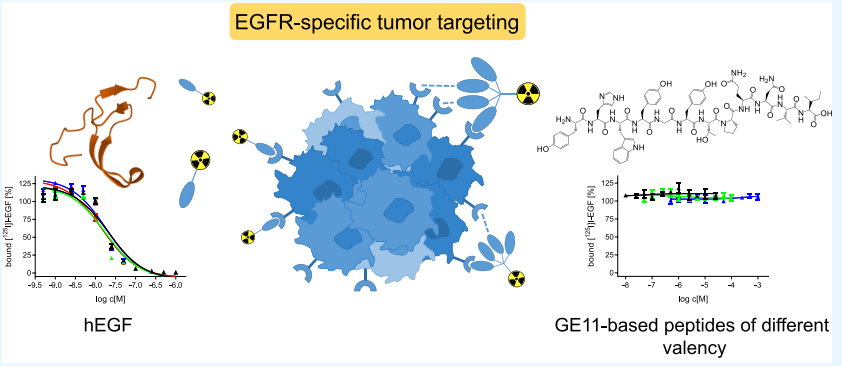

ABSTRACT: The epidermal growth factor receptor (EGFR) is closely associated with tumor development and progression and thus an important target structure for imaging and therapy of various tumors. As a result of its important role in malignancies of various origins and the fact that antibody-based compounds targeting the EGFR have significant drawbacks in terms of *in vivo* pharmacokinetics, several attempts have been made within the last five years to develop peptide-based EGFR-specific radioligands based on the GE11 scaffold. However, none of these approaches have shown convincing results so far, which has been proposed to be attributed to different potential challenges associated with the GE11 lead structure: first, an aggregation of radiolabeled peptides, which might prevent their interaction with their target receptor, or second, a relatively low affinity of monomeric GE11, necessitating its conversion into a multimeric or polymeric form to achieve adequate EGFR-targeting properties. In the present work, we investigated if these aforementioned points are indeed critical and if the EGFR-targeting ability of GE11 can be improved by choosing an appropriate hydrophilic molecular design or a peptide multimer system to obtain a promising radiopeptide for the visualization of EGFR-overexpressing malignancies by positron emission tomography (PET). For this purpose, we developed several monovalent ^{68}Ga-labeled GE11-based agents, a peptide homodimer and a homotetramer to overcome the challenges associated with GE11. The developed ligands were successfully labeled with $^{68}Ga^{3+}$ in high radiochemical yields of ≥97% and molar activities of 41−104 GBq/μmol. The resulting radiotracers presented $\log_{D(7.4)}$ values between −2.17 ± 0.21 and −3.79 ± 0.04 as well as a good stability in human serum with serum half-lives of 112 to 217 min for the monovalent radiopeptides and 84 and 62 min for the GE11 homodimer and homotetramer, respectively. In the following *in vitro* studies, none of the ^{68}Ga-labeled radiopeptides demonstrated a considerable EGF receptor-specific uptake in EGFR-positive A431 cells. Moreover, none of the agents was able to displace [^{125}I]I-EGF from the EGFR in competitive displacement assays in the same cell line in concentrations of up to 1 mM, whereas the endogenous receptor ligand hEGF demonstrated a high affinity of 15.2 ± 3.3 nM. These results indicate that it is not the aggregation of the GE11 sequence that seems to be the factor limiting the usefulness of the peptide as basis for radiotracer design but the limited affinity of monovalent and small homomultivalent GE11-based radiotracers to the EGFR. This highlights that the development of small-molecule GE11-based radioligands is not promising.

INTRODUCTION

The epidermal growth factor receptor (EGFR), also termed as the human epidermal growth factor receptor (HER1), is part of the EGF receptor family comprising, besides the EGFR, three other important members, namely, HER2−HER4. All receptors of this family exert important functions in cell physiology as they regulate protein transcription, proliferation, cell cycle pro-

Received: June 1, 2022
Accepted: July 15, 2022
Published: July 28, 2022

gression, apoptosis and cell differentiation, for example.[1−3] Dysregulation of the EGF receptor family is closely associated with oncogenesis and cancer progression. Especially, the EGFR is involved in different cancer-promoting processes such as the induction of anti-apoptotic effects, tumor cell proliferation, angiogenesis, increased cell motility, and metastatic growth.[1,4,5] Furthermore, it represents one of the most frequently altered oncogenes in solid cancer.[6] Thus, EGFR upregulation can be found in many human cancers such as colorectal, lung, breast, prostate, head and neck, liver, ovary, and esophageal cancer as well as gliomas and glioblastoma.[3,6−8]

Due to its high relevance in cancer development and progression, the EGFR is an attractive target for radionuclide-based imaging and therapy of malignancies.[1,4] In the case of tumor imaging with positron emission tomography (PET) and single photon emission computed tomography (SPECT), different EGFR-specific carrier molecules have been introduced to achieve a cancer cell-specific accumulation of the radiotracer, mostly based on highly receptor-specific proteins such as full-length antibodies in the IgG format or antibody fragments in the $F(ab')_2$, Fab, or $(scFv)_2$ format.[4] Despite high target affinity and specificity, the application of antibodies and other large proteins results in several problems for imaging, namely, a long circulation, limited tissue penetration, and slow pharmacokinetic profile, entailing slow clearance from background organs and tumor uptakes, limiting tumor-to-background contrasts especially at early time points. Furthermore, the enhanced permeability and retention (EPR) effect can lead to an unspecific uptake into tumor lesions and decreases imaging sensitivity and specificity. In contrast, smaller molecules such as peptides usually show fast pharmacokinetics and efficient tissue penetration while enabling a high target affinity and specificity. Furthermore, they can be easily synthesized, chemically modified, and adapted to the specific needs in molecular design, making them ideal candidates for the development of EGFR-specific radiotracers. Therefore, it is not surprising that in the last, approximately, 5 years, there has been increased effort to develop peptide-based radiotracers suitable for sensitive and specific imaging of the EGFR.

Most of these compounds were based on the peptide GE11 (Figure 1) as an EGFR-specific lead. GE11 was identified as a

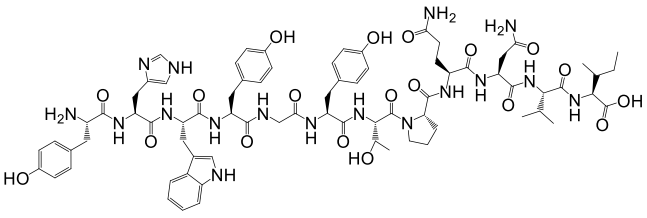

Figure 1. Structure of the EGFR-specific peptide GE11.

potential EGFR-specific peptide in 2005 by phage display and was shown to bind with a K_d of 22.3 ± 0.4 nM to the EGFR and in the same position as the physiological ligand hEGF.[9] GE11 was furthermore repeatedly reported to be a promising carrier of cancer therapeutics to EGFR-positive tumor cells.[5]

As a result, several groups have reported the development of GE11-based radiotracers over the past five years. Some of these comprised γ emitters such as ^{99m}Tc and ^{111}In for application in SPECT imaging,[10−13] but most of the attempts focused on the development of PET radiotracers comprising β^+ emitters such as ^{18}F, ^{68}Ga, ^{64}Cu, and ^{124}I.[12,14−17] Although some of the studies only described the synthesis and radiosynthesis of the radioligands without evaluating them *in silico*, *in vitro*, or *in vivo*, several agents were also studied *in vivo* in tumor-bearing mice. In these studies, some consistent features with respect to *in vivo* pharmacokinetics, tumor uptakes, and organ distribution of the radiotracers were observed: (i) their primarily renal excretion, (ii) relatively low tumor accumulation with resulting low tumor-to-muscle ratios of 3−3.5 within the observation period of 2−4 h post injection, and (iii) an only moderately blockable accumulation ranging from $^1/_3$ to about $^1/_2$ of the uptake into the tumor, raising doubts about a high EGFR specificity of the radioligands.[10,11,13,14,17] At best, the pharmacokinetic characteristics of the radioligands enabled only suboptimal visualization of the corresponding tumors.

A recent well-designed study by Striese et al.[17] attempted to systematically study and explain these frequently described phenomena of unfavorable *in vivo* properties of GE11-based diagnostic radiotracers and proposed the following theories. First, they inferred from their own results and those found in the literature that the peptide itself may be prone to aggregation, which would limit the interaction probability of the peptide with the target receptor explaining the unfavorable tumor uptake pattern of the radioligands. It was hypothesized that the introduction of hydrophilic linkers between peptide and radiolabel might improve the pharmacokinetic properties of the radiotracers. Furthermore, it was determined that the targeting agents successfully binding to the EGFR were based on constructs comprising many copies of the peptide. Thus, a sufficiently strong EGFR interaction might be present only in the case of using GE11 multimers or polymers as targeting units, whereas the application of a monovalent GE11 peptide would consequently result in a very limited target affinity. This assumption is supported by a recent study by Abourbeh et al.[18] who systematically investigated the EGFR-targeting properties of GE11 in monomeric and polymeric forms. In contrast, the endogenous ligand hEGF showed a very high EGFR affinity under the same conditions.

As there are only few studies available on the development of EGFR-specific radiotracers based on the GE11 peptide lead and all of them showing suboptimal results, we aimed here to test the abovementioned hypotheses on potential limitations in molecular design of GE11-based radiopeptides. For this purpose, we created a set of several different monovalent hydrophilic chelator-modified GE11 peptides as well as two multivalent GE11 analogues in order to systematically determine the influence of molecular design on the properties of the resulting radiotracers. The developed agents were radiolabeled with $^{68}Ga^{3+}$ and evaluated regarding their hydrophilicity/lipophilicity profile and their stability toward peptidase degradation in human serum. Further, the substances were also evaluated *in vitro* regarding their uptake into EGFR-positive A431 cells and in competitive displacement assays in the same cell line to determine their EGFR affinity. We aimed at answering the question whether an increased peptide hydrophilicity or valency can improve the EGFR-targeting properties of GE11 and identifying the most appropriate approach toward potent GE11-based radiopeptides.

MATERIALS AND METHODS

General. *Chemicals, Radiochemicals, and Materials for in Vitro Assays.* All chemicals were purchased from commercial sources in analytical grade quality and used without further purification unless otherwise stated. Fmoc- and side chain-

https://doi.org/10.1021/acsomega.2c03407
ACS Omega 2022, 7, 27690−27702

protected amino acids and all resins (Fmoc-Ile-Wang resin LL (100−200 mesh) (loading 0.31−0.40 mmol/g), Rink Amide MBHA resin LL (100−200 mesh) (loading 0.36 mmol/g), Rink Amide AM resin LL (100−200 mesh) (loading 0.36 mmol/g), NovaPEG Rink Amide resin LL (loading 0.15−0.25 mmol/g), and benzotriazol-1-yloxytripyrrolidinophosphonium hexafluorophosphate (PyBOP)) were purchased from NovaBiochem (Darmstadt, Germany). Bis(2,5-dioxopyrrolidin-1-yl) 4,7,10,13,16,19-hexaoxadocosanedioate (PEG_5-bis-NHS ester) was purchased from Broadpharm (San Diego, USA), tetrakis-(triphenylphosphine)palladium(0) ($Pd(PPh_3)_4$) from TCI (Eschborn, Germany), and 4-(4,7-bis(2-(*t*-butoxy)-2-oxoethyl)-1,4,7-triazacyclononan-1-yl)-5-(*tert*-butoxy)-5-oxo-pentanoic acid ((*R*)-NODA-GA(tBu)$_3$) from CheMatech (Dijon, France). 8-(9-Fluorenylmethyl-oxycarbonyl-amino)-3,6-dioxaoctanoic acid (PEG_1, Fmoc-NH-PEG_1-COOH), 15-(9-fluorenylmethyloxycarbonyl)amino-4,7,10,13-tetraoxapentadecanoic acid (PEG_3, Fmoc-NH-PEG_3-COOH), 21-(9-fluorenylmethyloxycarbonyl)amino-4,7,10,13,16,19-hexaoxaheneicosanoic acid (PEG_5, Fmoc-NH-PEG_5-COOH), 1-(9-fluorenylmethyloxycarbonyl)amino-3,6,9,12,15,18,21,24-octaoxaheptacosan-27-oic acid (PEG_7, Fmoc-NH-PEG_7-COOH), and 2-(bis(3-(((9*H*-fluoren-9-yl)methoxy)-carbonylamino)-propyl)-amino)-acetic acid potassium hemisulfate ((Fmoc-NH-Propyl)$_2$Gly-OH × $KHSO_4$) were obtained from Iris Biotech (Marktredwitz, Germany). Dichloromethane (DCM), diethylether, dimethylformamide (DMF), piperidine, 2-(1*H*-benzotriazol-1-yl)-1,1,3,3-tetramethyluronium hexafluorophosphate (HBTU), trifluoroacetic acid (TFA), and water were purchased from Carl Roth (Karlsruhe, Germany), acetonitrile (MeCN) from Häberle Labortechnik (Lonsee-Ettlenschieß, Germany), and *N*,*N*-diisopropylethylamine (DIPEA) and triisopropylsilane (TIS) from Sigma-Aldrich (Taufkirchen, Germany). Formic acid was obtained from Thermo Fisher Scientific (Schwerte, Germany). Human serum (pooled serum from male AB clotted whole blood) was also purchased from Sigma-Aldrich (Taufkirchen, Germany). A431 epidermoid carcinoma cells were obtained from DSMZ (Braunschweig, Germany) and cell culture media from Bio & Sell (Feucht, Germany). [^{125}I]I-EGF in a molar activity of 81.4 TBq/mmol was obtained from PerkinElmer as custom synthesis (NEX083000MC, Rodgau, Germany). [^{68}Ga]$GaCl_3$ for ^{68}Ga radiolabeling reactions was obtained from an IGG100 ^{68}Ge/^{68}Ga generator system (Eckert & Ziegler, Berlin, Germany). H_2O (Tracepur quality), hydrochloric acid (30%, Suprapur quality), and sodium hydroxide (30%, Suprapur quality) for radiolabeling reactions were purchased from Merck (Darmstadt, Germany).

Instrumentation. HPLC: For HPLC chromatography, a Dionex UltiMate 3000 system was used together with Chromeleon Software (version 6.80). For analytical chromatography and semipreparative analyses, a Chromolith Performance (RP-18e, 100−4.6 mm, Merck, Germany) and Chromolith SemiPrep (RP-18e, 100−10 mm, Merck, Germany) columns were used, respectively. For radioanalytical chromatography, a Dionex UltiMate 3000 system equipped with a Raytest GABI Star radioactivity detector was used together with a Chromolith Performance (RP-18e, 100−4.6 mm, Merck, Germany) column. All operations were performed with a flow rate of 4 mL/min using H_2O (supplemented with 0.1% TFA or formic acid) and MeCN (also supplemented with 0.1% TFA or formic acid) as solvents. The gradient used for analytical and radioanalytical chromatography was typically 0−100% MeCN within 5 min, whereas gradients for semipreparative chromatography were chosen individually and are reported in the respective synthesis section. MALDI-TOF MS: Matrix-assisted laser desorption/ionization (MALDI) time-of-flight mass spectra were obtained utilizing a Bruker Daltonics Microflex spectrometer (linear acquisition mode, positive ion source, and 200 shots per spot). α-Cyano-4-hydroxycinnamic acid (α-CS) or 2,5-dioxybenzoic acid (GS) was chosen as the matrix, and the dried-droplet method was used for sample preparation on a microscout target (MSP 96 target polished steel BC, Bruker Daltonics, Germany). The data were recorded with flexControl version 3.3 and analyzed with flexAnalysis version 3.3 software. HR-ESI-MS: For high-resolution electrospray ionization mass spectroscopy (HR-ESI-MS), a Thermo Finnigan LTQ FT Ultra Fourier Transform Ion Cyclotron Resonance (Dreieich, Germany) mass spectrometer was used. The resolution was adjusted to 100.000 at m/z 400. Depending on the sample, a mass range of 50−2000 u was chosen. The spray capillary voltage at the IonMax ESI-nozzle was 4 kV, the temperature of the heater capillaries was 250 ° C, the nitrogen sheath gas flow was 20, and the sweep gas flow was 5 units. Flow injection analysis (FIA/ESI) utilized a surveyor MS pump at a flow rate of 100 μL/min with 20/80% (v/v) or 80/20% (v/v) water/acetonitrile as solvent. A volume of 1−10 μL of the sample was injected under use of an inline filter. γ counter: γ counting was performed using a 2480 Wizard gamma counter system from PerkinElmer. Ultrasonic bath: Ultrasound-assisted syntheses were performed in a Bandelin Sonorex Super RK 225 H ultrasonic bath (Berlin, Germany) with the temperature of the water kept at ambient temperature.

Peptide Syntheses. Solid-phase peptide synthesis (SPPS) was performed according to standard Fmoc protocols[19] in standard syringes (5 mL, HSW, Tuttlingen, Germany) equipped with 35 μm porous high-density polyethylene frits (Reichelt Chemietechnik, Heidelberg, Germany). Two different methods were used for coupling, namely, mechanical agitation, where reactions were carried out in DMF for 60 min on a shaker at ambient temperature using 4 equiv of the respective amino acid and 3.9 equiv of HBTU as the coupling reagent with 4 equiv of DIPEA as the base, and ultrasound-assisted couplings, where reactions were carried out in DMF for 15 min in an ultrasonic bath at ambient temperature using 2 equiv of the respective amino acid and 1.9 equiv of HBTU as the coupling reagent with 2 equiv of DIPEA as the base. Fmoc-protecting groups were removed using 50% piperidine in DMF (v/v) (2 and 5 min). Cleavage from the resin and simultaneous removal of acid-labile protecting groups was performed with a mixture of TFA, TIS, and H_2O ($v/v/v$ 95/2.5/2.5) for 2−3 h at room temperature followed by evaporation of the volatile materials. The residue was dissolved in 1:1 MeCN/H_2O + 0.1% TFA (v/v), purified by semipreparative HPLC, and subsequently lyophilized. HR-ESI-MS spectra of **1**−**7** and **9**−**11** can be found in the Supporting Information (Figures S1−S10).

*NODA-GA-PEG_1-GE11 (**1**).* NODA-GA-PEG_1-Tyr-His-Trp-Tyr-Gly-Tyr-Thr-Pro-Gln-Asn-Val-Ile (**1**) was synthesized on solid support according to standard amino acid coupling protocols on a commercially available Fmoc-Ile-Wang resin LL (100−200 mesh, loading 0.31−0.40 mmol/g), standard N_α-Fmoc amino acids, HBTU as a coupling reagent, Fmoc-NH-PEG_1-COOH, and (*R*)-NODA-GA(tBu)$_3$. The cleavage of the crude product from the solid support and the simultaneous removal of acid-labile protecting groups were performed using a mixture of TFA, TIS, and H_2O ($v/v/v$ 95/2.5/2.5) for 3 h at room temperature followed by evaporation of the volatile

https://doi.org/10.1021/acsomega.2c03407
ACS Omega 2022, 7, 27690−27702

materials. The crude product was dissolved in 1:1 MeCN/H_2O + 0.1% TFA (v/v), purified by semipreparative HPLC, and subsequently isolated as a colorless solid after lyophilization. Gradient: 0−80% MeCN + 0.1% formic acid in 10 min (R_t = 5.4 min), yield: 17%. MALDI-TOF-MS (m/z) using α-cyano-4-hydroxycinnamic acid as the matrix substance for $[M + H]^+$ (calculated): 2042.47 (2043.24), $[M + Na]^+$ (calculated): 2064.53 (2065.22), $[M + K]^+$ (calculated): 2080.40 (2081.33). MALDI-TOF-MS (m/z) using 2,5-dihydroxybenzoic acid as the matrix substance for $[M + H]^+$ (calculated): 2042.37 (2043.24), $[M + Na]^+$ (calculated): 2065.35 (2065.22), $[M + K]^+$ (calculated): 2080.61 (2081.33). HR-ESI-MS (m/z) $[M + 2H]^{2+}$ (calculated): 1021.9756 (1022.1250), $[M + H + Na]^{2+}$ (calculated): 1032.9699 (1033.1159), $[M - 2H]^{2-}$ (calculated): 1019.9651 (1020.1090).

*NODA-GA-PEG$_3$-GE11 (**2**).* NODA-GA-PEG$_3$-Tyr-His-Trp-Tyr-Gly-Tyr-Thr-Pro-Gln-Asn-Val-Ile (**2**) was synthesized on solid support according to standard amino acid coupling protocols on a commercially available Fmoc-Ile-Wang resin LL (100−200 mesh, loading 0.31 mmol/g), standard N_α-Fmoc amino acids, HBTU as a coupling reagent, Fmoc-NH-PEG$_3$-COOH, and (R)-NODA-GA(tBu)$_3$. The cleavage of the crude product from the solid support and the simultaneous removal of acid-labile protecting groups were performed using a mixture of TFA, TIS, and H_2O ($v/v/v$ 95/2.5/2.5) for 3 h at room temperature followed by evaporation of the volatile materials. The crude product was dissolved in 1:1 MeCN/H_2O + 0.1% TFA (v/v), purified by semipreparative HPLC, and subsequently isolated as a colorless solid after lyophilization. Gradient: 20−80% MeCN + 0.1% formic acid in 8 min (R_t = 3.06 min), yield: 26%. MALDI-TOF-MS (m/z) using α-cyano-4-hydroxycinnamic acid as the matrix substance for $[M + H]^+$ (calculated): 2145.25 (2145.38), $[M + Na]^+$ (calculated): 2166.31 (2167.36), $[M + K]^+$ (calculated): 2182.84 (2183.47). MALDI-TOF-MS (m/z) using 2,5-dihydroxybenzoic acid as the matrix substance for $[M + H]^+$ (calculated): 2145.46 (2145.38), $[M + Na]^+$ (calculated): 2167.54 (2167.36), $[M + K]^+$ (calculated): 2183.50 (2183.47). HR-ESI-MS (m/z) $[M + 2H]^{2+}$ (calculated): 1073.0099 (1073.1915), $[M + H + Na]^{2+}$ (calculated): 1084.0044 (1084.1824), $[M - 2H]^{2-}$ (calculated): 1070.9991 (1071.1755).

*NODA-GA-PEG$_5$-GE11 (**3**).* NODA-GA-PEG$_5$-Tyr-His-Trp-Tyr-Gly-Tyr-Thr-Pro-Gln-Asn-Val-Ile (**3**) was synthesized on solid support according to standard amino acid coupling protocols and ultrasound-assisted synthesis instead of mechanical agitation on a commercially available Fmoc-Ile-Wang resin LL (100−200 mesh, loading 0.31−0.40 mmol/g), standard N_α-Fmoc amino acids, HBTU as a coupling reagent, Fmoc-NH-PEG$_5$-COOH, and (R)-NODA-GA(^{t}Bu)$_3$. The cleavage of the crude product from the solid support and the simultaneous removal of acid-labile protecting groups were performed using a mixture of TFA, TIS, and H_2O ($v/v/v$ 95/2.5/2.5) for 3 h at room temperature followed by evaporation of the volatile materials. The crude product was dissolved in 1:1 MeCN/H_2O + 0.1% TFA (v/v), purified by semipreparative HPLC, and subsequently isolated as a colorless solid after lyophilization. Gradient: 10−40% MeCN +0.1% TFA in 8 min (R_t = 5.14 min), yield: 50%. MALDI-TOF-MS (m/z) using α-cyano-4-hydroxycinnamic acid as the matrix substance for $[M + H]^+$ (calculated): 2233.76 (2233.48). HR-ESI-MS (m/z) $[M + 2H]^{2+}$ (calculated): 1117.0394 (1117.2445), $[M - 2H]^{2-}$ (calculated): 1114.5187 (1115.2285), $[M - 4H + 3K]^{2-}$ (calculated): 1171.8424 (1172.8680).

*NODA-GA-PEG$_7$-GE11 (**4**).* NODA-GA-PEG$_7$-Tyr-His-Trp-Tyr-Gly-Tyr-Thr-Pro-Gln-Asn-Val-Ile (**4**) was synthesized on solid support according to standard amino acid coupling protocols on a commercially available Fmoc-Ile-Wang resin LL (100−200 mesh, loading 0.31 mmol/g), standard N_α-Fmoc amino acids, HBTU as a coupling reagent, Fmoc-NH-PEG$_7$-COOH, and (R)-NODA-GA(tBu)$_3$. The cleavage of the crude product from the solid support and the simultaneous removal of acid-labile protecting groups were performed using a mixture of TFA, TIS, and H_2O ($v/v/v$ 95/2.5/2.5) for 3 h at room temperature followed by evaporation of the volatile materials. The crude product was dissolved in 1:1 MeCN/H_2O + 0.1% TFA (v/v), purified by semipreparative HPLC, and subsequently isolated as a colorless solid after lyophilization. Gradient: 0−80% MeCN + 0.1% TFA in 8 min (R_t = 3.54 min), yield: 27%. MALDI-TOF MS (m/z) using α-cyano-4-hydroxycinnamic acid as the matrix substance for $[M + H]^+$ (calculated): 2321.34 (2321.59), $[M + Na]^+$ (calculated): 2342.57 (2343.57), $[M + K]^+$ (calculated): 2358.50 (2359.68). MALDI-TOF-MS (m/z) using 2,5-dihydroxybenzoic acid as the matrix substance for $[M + H]^+$ (calculated): 2321.45 (2321.59), $[M + Na]^+$ (calculated): 2343.34 (2343.57), $[M + K]^+$ (calculated): 2358.61 (2359.68). HR-ESI-MS (m/z) $[M + 2H]^{2+}$ (calculated): 1161.0621 (1161.2975), $[M + H + Na]^{2+}$ (calculated): 1172.0567 (1172.2884), $[M - 2H]^{2-}$ (calculated): 1159.0520 (1159.2815).

*NODA-GA-Asp-Gly-Asp-PEG$_3$-GE11 (**5**).* NODA-GA-Asp-Gly-Asp-PEG$_3$-Tyr-His-Trp-Tyr-Gly-Tyr-Thr-Pro-Gln-Asn-Val-Ile (**5**) was synthesized on solid support according to standard amino acid coupling protocols on a commercially available Fmoc-Ile-Wang resin LL (100−200 mesh, loading 0.31 mmol/g), standard N_α-Fmoc amino acids, HBTU as the coupling reagent, Fmoc-NH-PEG$_7$-COOH, and (R)-NODA-GA(tBu)$_3$. The cleavage of the crude product from the solid support and the simultaneous removal of acid-labile protecting groups were performed using a mixture of TFA, TIS, and H_2O ($v/v/v$ 95/2.5/2.5) for 3 h at room temperature followed by evaporation of the volatile materials. The crude product was dissolved in 1:1 MeCN/H_2O + 0.1% TFA (v/v), purified by semipreparative HPLC, and subsequently isolated as a colorless solid after lyophilization. Gradient: 0−60% MeCN + 0.1% formic acid in 10 min (R_t = 6.40 min), yield: 14%. MALDI-TOF MS (m/z) using α-cyano-4-hydroxycinnamic acid as the matrix substance for $[M + H]^+$ (calculated): 2432.06 (2432.60), $[M + Na]^+$ (calculated): 2454.02 (2454.08), $[M + K]^+$ (calculated): 2470.79 (2470.69). MALDI-TOF-MS (m/z) using 2,5-dihydroxybenzoic acid as the matrix substance for $[M + H]^+$ (calculated): 2432.61 (2432.60), $[M + Na]^+$ (calculated): 2454.69 (2454.08), $[M + K]^+$ (calculated): 2471.24 (2470.69). HR-ESI-MS (m/z) $[M + 2H]^{2+}$ (calculated): 1216.3672 (1216.8055), $[M + H + Na]^{2+}$ (calculated): 1227.5397 (1227.7964), $[M - 3H]^{3-}$ (calculated): 809.3551 (809.5237).

*GE11 Homodimer (**6**).* To a solution of the NODA-GA-bis-amino dendron (**9**) (2.2 mg, 2.4 μmol) in absolute DMF (1 mL) were added DIPEA (15 equiv, 6 μL) and GE11-PEG$_5$-NHS ester (**11**) (2.6 equiv, 12.5 mg, 6.2 μmol), and the reaction was conducted in the ultrasonic bath. The reaction progress was monitored by analytical HPLC and was found to be complete within 15 min. The product was purified by semipreparative HPLC and subsequently isolated as a colorless solid after lyophilization. Gradient: 20−40% MeCN + 0.1% TFA in 8 min (R_t = 5.84 min), yield: 23%. MALDI-TOF-MS (m/z) using α-cyano-4-hydroxycinnamic acid as the matrix substance for [M +

https://doi.org/10.1021/acsomega.2c03407
ACS Omega 2022, 7, 27690−27702

H]$^{+}$ (calculated): 4701.08 (4694.29). HR-ESI-MS (m/z) [M + 4H]$^{4+}$ (calculated): 1174.0890 (1174.3285), [M + 3H]$^{3+}$ (calculated): 1565.1184 (1565.4353).

*GE11 Homotetramer (**7**).* To a solution of the NODA-GA-tetra-amino dendron (**10**) (3.0 mg, 2.4 μmol) in absolute DMF (1 mL) were added DIPEA (15 equiv, 6 μL) and GE11-PEG$_6$-NHS ester (**11**) (4.6 equiv, 11.0 μmol, 22.0 mg), and the reaction was conducted in the ultrasonic bath. The reaction progress was monitored by analytical HPLC and was found to be complete within 60 min. The product was purified by semipreparative HPLC and subsequently isolated as a colorless solid after lyophilization. Gradient: 30−40% MeCN + 0.1% TFA in 8 min (R_t = 2.94 min), yield: 20%. MALDI-TOF-MS (m/z) using α-cyano-4-hydroxycinnamic acid as matrix substance for [M + 2Na]$^{+}$ (calculated): 8852.25 (8853.93). HR-ESI-MS (m/z) [M + 7H]$^{7+}$ (calculated): 1259.2019 (1259.2863), [M + 6H]$^{6+}$ (calculated): 1468.9013 (1468.9993), [M + 5H]$^{5+}$ (calculated): 1762.4770 (1762.5976).

*NODA-GA-bis-amino Dendron (**9**).* The NODA-GA-bis-amino dendron (**9**) was synthesized according to standard solid phase-based synthesis methods by coupling Fmoc-Lys(Mtt)-OH and Fmoc-PEG$_3$-OH to a standard Rink amide resin. Using 1% TFA in DCM (v/v) 3 × 15 min, the Mtt-protecting group of the lysine was removed and (R)-NODA-GA(tBu)$_3$ (excess: 2 equiv instead of 4) was coupled to the ε-amino functionality of the lysine, utilizing PyBOP instead of HBTU (excess: 1.9 equiv instead of 3.9) as a coupling reagent and prolonged reaction times of 30 min / 2.5 h (ultrasound-assisted/mechanical). Afterward, (Fmoc-NH-Propyl)$_2$Gly-OH × KHSO$_4$ was coupled by applying standard conditions but prolonged reaction times of 30 min/2.5 h (ultrasound-assisted/mechanical) to the amino functionality of the PEG$_3$-linker. Cleavage from the resin and simultaneous removal of the acid-labile tBu-protecting groups were performed using a mixture of TFA, TIS, and H$_2$O ($v/v/v$; 95/2.5/2.5) for 3 h at room temperature followed by evaporation of the volatile materials. The resulting residue was dissolved in 1:1 MeCN/H$_2$O + 0.1% TFA (v/v), purified by semipreparative HPLC, and subsequently isolated as a colorless hardening oil after lyophilization. Gradient: 0−40% MeCN + 0.1% TFA in 8 min (R_t = 4.13 min), yield: 78 / 45% (ultrasound-assisted/mechanical). MALDI-TOF-MS (m/z) using α-cyano-4-hydroxycinnamic acid as matrix substance for [M + H]$^{+}$ (calculated): 921.52 (921.56). HR-ESI-MS (m/z) [M + H]$^{+}$ (calculated): 921.5616 (921.5615), [M + 2H]$^{2+}$ (calculated): 461.2843 (461.5600).

*NODA-GA-tetra-amino Dendron (**10**).* NODA-GA-tetra-amino-dendron (**10**) was synthesized following the same protocols used for the synthesis of **9**. Fmoc-Lys(Mtt)-OH and Fmoc-PEG$_3$-OH were coupled to Rink amide resin followed by Mtt-protecting group removal using 1% TFA in DCM (v/v) for 3 × 15 min. (R)-NODA-GA(tBu)$_3$ (excess: 2 equiv instead of standard 4 equiv) was coupled to the ε-amino functionality of the lysine, utilizing PyBOP (excess: 1.9 equiv instead of 3.9) as a coupling reagent and prolonged reaction times of 30 min by ultrasound-assisted synthesis. (Fmoc-NH-Propyl)$_2$Gly-OH × KHSO$_4$ was coupled twice using 2 equiv of the synthon in the first reaction step and 6 equiv during the second reaction step and prolonged reaction times of 30 min for ultrasound-assisted synthesis. Cleavage from the resin and simultaneous removal of the acid-labile tBu-protecting groups were performed using a mixture of TFA, TIS, and H$_2$O ($v/v/v$ 95/2.5/2.5) for 3 h at room temperature followed by evaporation of the volatile materials. The resulting residue was dissolved in 1:1 MeCN/H$_2$O + 0.1% TFA (v/v), purified by semipreparative HPLC, and subsequently isolated as a colorless hardening oil after lyophilization. Gradient: 0−40% MeCN + 0.1% TFA in 8 min (R_t = 4.67 min), yield: 72%. MALDI-TOF-MS (m/z) using α-cyano-4-hydroxycinnamic acid as the matrix substance for [M + H]$^{+}$ (calculated): 1263.22 (1263.84). HR-ESI-MS (m/z) [M + H]$^{+}$ (calculated): 1263.8382 (1263.8364).

*GE11-PEG$_5$-NHS Ester (**11**).* The GE11-PEG$_5$-NHS ester (**11**) (NHS-PEG$_5$-Tyr-His-Trp-Tyr-Gly-Tyr-Thr-Pro-Gln-Asn-Val-Ile) was synthesized on solid support according to standard protocols using a commercially available Fmoc-Ile-Wang resin LL (100−200 mesh, loading 0.31−0.40 mmol/g), HBTU as a coupling reagent, and standard N$_\alpha$-Fmoc amino acids and bis-PEG$_5$-NHS ester as agents. The conjugation of the bis-PEG$_5$-NHS ester (8 equiv) was performed without prior activation with HBTU but under DIPEA assistance (4 equiv) for 1 h using mechanical agitation. The cleavage of the crude product from the solid support and the simultaneous removal of acid-labile protecting groups were performed with a mixture of TFA, TIS, and H$_2$O ($v/v/v$ 95/2.5/2.5) for 3 h at room temperature followed by evaporation of the volatile materials. The crude product was dissolved in 1:1 MeCN/H$_2$O + 0.1% TFA (v/v), purified by semipreparative HPLC, and subsequently isolated as a colorless solid after lyophilization. Gradient: 0−60% MeCN + 0.1% TFA in 8 min (R_t = 6.36 min), yield: 46%. MALDI-TOF-MS (m/z) using α-cyano-4-hydroxycinnamic acid as the matrix substance for [M + H]$^{+}$ (calculated): 2001.91 (2003.17). HR-ESI-MS (m/z) [M + 2H]$^{2+}$ (calculated): 1001.4607 (1001.5865).

*^{68}Ga Radiolabeling of **1**−**7**.* For radiolabeling with ^{68}Ga^{3+}, [^{68}Ga]GaCl$_3$ was obtained by fractioned elution of a commercial ^{68}Ge/^{68}Ga generator system (IGG100 system, Eckert & Ziegler) with 0.1 M hydrochloric acid (HCl). A solution of the peptide derivatives **1**−**7** (1−20 nmol) in H$_2$O (Tracepur quality, 1−20 μL) was added to 50−250 MBq [^{68}Ga]GaCl$_3$ (0.5 mL), and the pH was adjusted to 3.5−4.0 by addition of sodium acetate solution (1.25 M, 100−150 μL). After a 10 min reaction at 45−50 °C, samples were analyzed by radio-HPLC. The radiolabeled products were found to be 98−100% pure and obtained in non-optimized molar activities of 80−104 GBq/μmol.

*Determination of log$_{D(7.4)}$ Values for [^{68}Ga]Ga-**1** to [^{68}Ga]Ga-**7**.* The water$_{pH7.4}$/1-octanol partition coefficient (log$_{D(7.4)}$) of the developed radiotracers was determined by addition of a solution of the respective radiolabeled peptide (5 μL, 0.5−2 MBq) to a mixture of 1-octanol (800 μL) and phosphate buffer (0.05 M, pH 7.4, 795 μL). The mixtures were vigorously shaken for 5 min on a mechanical shaker and subsequently centrifuged at 13,000 rpm for 2 min to achieve complete phase separation. A volume of 125 μL of each phase was taken, and the amount of radioactivity in each phase was determined by γ counting. Experiments were performed thrice, each in triplicate.

*Determination of the Stability of [^{68}Ga]Ga-**1** to [^{68}Ga]Ga-**7** in Human Serum.* A sample of the respective radiolabeled peptide (125 μL, 10−30 MBq, pH 7.4) was added to human serum (500 μL) and warmed to 37 °C. At defined time points (t = 0, 5, 15, 30, 45, 60, and 90 min), 75 μL of the mixture was added to ice-cold ethanol, further cooled on ice for 5 min, and centrifuged at 13,000 rpm for 90 s. The supernatant was collected, the activity of the supernatant and the precipitate measured, and whereafter, the supernatant was analyzed by

https://doi.org/10.1021/acsomega.2c03407
ACS Omega 2022, 7, 27690−27702

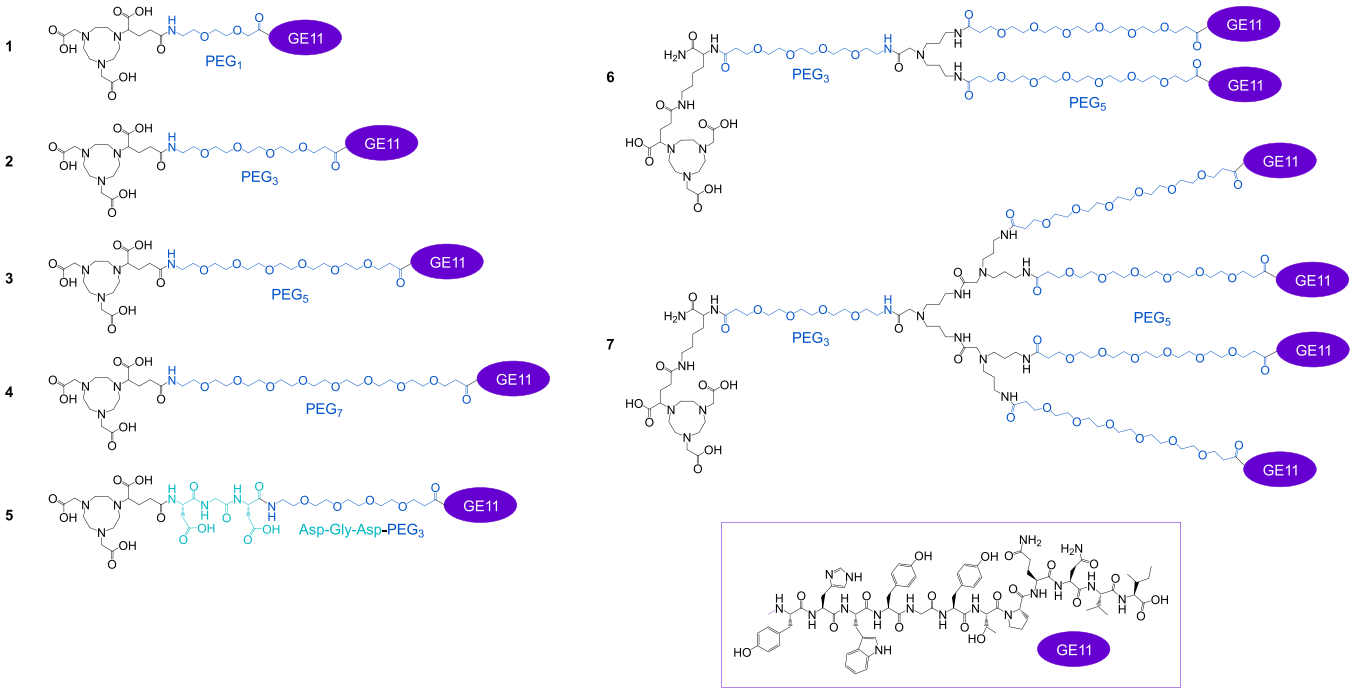

Figure 2. Depiction of the chemical structures of the developed monovalent GE11-based agents **1**−**5**, the homodimer **6**, and the homotetramer **7**. Hydrophilic structure elements, namely, PEG linkers of different lengths and the additionally introduced Asp-Gly-Asp amino acid sequence, are depicted in dark and light blue, respectively.

radio-HPLC. Experiments were performed thrice for each radioligand.

Cell Culture. A431 epidermoid carcinoma cells were grown in DMEM, high glucose medium (Gibco) supplemented with 10% (*v*/*v*) fetal bovine serum and 1% (*v*/*v*) penicillin−streptomycin (10,000 U/mL) (Gibco) at 37 °C in a humidified CO_2 (5%) atmosphere and were split at >80% confluence.

Internalization Studies. A431 cells (10^6 per well) were seeded into 24-well cell culture multiwell plates (cellstar) and incubated for 2 days at 37 °C in a humidified CO_2 (5%) atmosphere. Immediately before the experiment, each well was washed twice with fresh internalization medium (DMEM, high glucose containing 1% fetal bovine serum) followed by the addition of internalization medium to a final volume of 1.35 mL per well. To half of the wells was added PBS containing 0.5% bovine serum albumin (BSA) (150 μL), while to the other half was added a blocking solution of a 100-fold molar excess of hEGF (5 nM) in PBS containing 0.5% bovine serum albumin solution (150 μL) followed by incubation at 37 °C for 10 min. Hereafter, a solution of the respective radiolabeled peptide (0.05 nM) in internalization medium (8 μL) was added to each well, and the plate was incubated at 37 °C for 30 min, 1 h, 2 h, or 3 h. Afterward, the medium was separated from the cells and each well was washed twice with 1 mL of an ice-cold internalization medium, and the washing solutions were added to the collected internalization medium (this combined solution represents the unbound fraction) and measured in a γ counter. To determine the surface-bound fraction, each well was incubated twice for 5 min with ice-cold glycine buffer (pH 2.8, 0.05 M, 1 mL) and the supernatants were collected and measured. The internalized fraction was determined by lysing the cells twice for 5 min with sodium hydroxide solution (2 M, 1 mL) and collection and measurement of the solutions. The amount of radiotracers in each fraction was determined by γ counting and referenced against a standard solution of the radiolabeled peptide (8 μL). Each experiment was performed thrice.

Competitive Displacement Studies. In vitro binding affinities were acquired by competitive displacement experiments with each performed in triplicate. MultiScreen$_{HTS}$-BV, 1 and 2 μm 96-well plates were incubated with PBS/BSA (1%) solution (200 μL per well) for 1 h before use. Each well was seeded with 10^5 A431 cells suspended in an Opti-MEM I (GlutaMAX I) medium, and the plate was incubated at 37 °C for 1 h with 0.25 kBq [^{125}I]I-EGF (25 μL) in the presence of 11 increasing concentrations ranging from 10^{-8} to 10^{-3} M of the respective competitor (**1**−**7**, 25 μL) or 5×10^{-10} to 10^{-6} M (hEGF) with one well empty ensuring 100% binding of the radioligand. After the incubation, the filters were washed three times with PBS (1×200 μL, 2×100 μL) to remove unbound [^{125}I]I-EGF, collected, and measured in a γ counter. The 50% inhibitory concentration (IC_{50}) values for each compound were obtained by nonlinear regression analysis using GraphPad Prism Software (v5.04). Each experiment was performed at least three times with each experiment being performed in triplicate.

RESULTS AND DISCUSSION

Synthesis of GE11-Based Radiolabeling Precursors 1−**7.** A set of several monovalent chelator-modified GE11 peptides (**1**−**5**) as well as two derivatives of higher valency (**6** and **7**, Figure 2) were developed and radiolabeled with $^{68}Ga^{3+}$. All compounds were finally evaluated toward their hydrophilicity and stability in human serum and *in vitro* toward their EGF receptor interaction properties. The monovalent agents comprised a NODA-GA ((1,4,7-triazacyclononane-4,7-diyl)-diacetic acid-1-glutaric acid) chelator for stable and efficient $^{68}Ga^{3+}$ and $^{64}Cu^{2+}$ radiolabeling[20,21] and hydrophilic PEG (polyethylene glycol) linkers of different lengths (**1**−**4**). The varying linker lengths result in different distances between the chelator/radiolabel and the peptide, which might have an

https://doi.org/10.1021/acsomega.2c03407
ACS Omega 2022, 7, 27690−27702

influence on the receptor interaction properties of the GE11 peptide carrier.[22,23] Further, the varying PEG linker length is supposed to result in changes in the hydrophilicity profiles of the agents[22,24] and thus might have an influence on a potential aggregation of the radiopeptides. Another derivative (**5**) was designed, which additionally comprised two negatively charged aspartic acids to further increase hydrophilicity and thus reduce potential radiopeptide aggregation. Previously, this approach was furthermore able to positively influence the *in vivo* pharmacokinetic profile of radiopeptides for tumor imaging.[25] In parallel, we also developed two GE11 derivatives of higher valency, namely, a GE11 dimer (**6**) and a respective tetramer (**7**), to investigate the influence of the peptide valency on the achievable EGFR affinities.

A further important advantage of using peptide multimers for targeting is their commonly increased metabolic stability compared to their monovalent counterparts, the resulting prolonged bioavailability of receptor-affine structures, and by this, their higher probability of a receptor interaction.[26,27] Multimers further usually exhibit increased avidities (avidity is the affinity of a multivalent binder to its target) to their target receptor compared to the respective monomers, which can be attributed to concomitant (and thus tighter) receptor binding and a higher probability of re-binding upon dissociation due to the "forced proximity effect" (Figure 3). These parameters

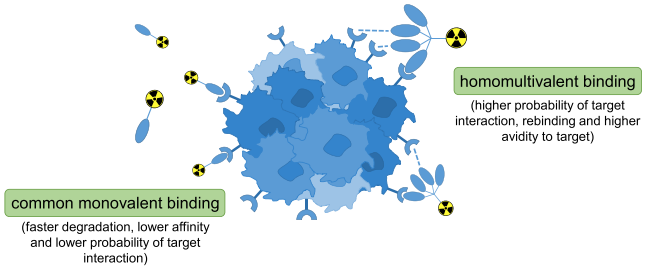

Figure 3. Schematic depiction of the receptor interaction characteristics of radiolabeled monovalent and multivalent peptides used for tumor targeting.

usually result in higher tumor uptakes combined with higher tumor-to-background ratios as well as prolonged tumor retention compared to the respective monovalent systems.[28−30]

For ligation of the molecular building blocks within the target agents, acid−amide bonds were chosen as they show high chemical stability and do not produce potential unintended effects of artificial structure elements such as susceptibility to certain chemical or physiological conditions or immunogenicity.

The monovalent peptide precursors **1**−**5** were synthesized by standard Fmoc-based solid phase peptide synthesis (SPPS) protocols[19] by successive conjugation of the required building blocks on an Ile-preloaded Wang resin. For this purpose, the NH-Fmoc- and side-chain-protected amino acids of the GE11 peptide sequence, Fmoc-PEG$_X$-OH linkers, additional amino acids (if applicable), and NODA-GA chelator in the form of its (*R*)-NODA-GA(*t*Bu)$_3$ derivative were successively coupled to the resin before the peptides were cleaved and simultaneously deprotected under acidic conditions. The schematic depiction of the synthesis process is shown in Scheme 1, and all monomers were obtained in moderate to good yields of 14−50%.

For the coupling of the activated building blocks, two different approaches were followed for some of the compounds: the standard mechanical agitation-aided conjugation and the ultrasound-assisted conjugation using a conventional ultrasonic bath. In contrast to the frequently used microwave-assisted peptide synthesis,[31] the application of ultrasound for more efficient coupling performance is still a rather new field.[32−34] Although all peptide syntheses were successful using both approaches, the ultrasound-assisted conjugation reactions required lower excesses of the activated building blocks (only 2 equiv instead of 4) and shorter reaction times to complete reactions (15 instead of 60 min for standard building blocks to be coupled), usually giving the products in considerably higher yields (1.5 to 2-fold).

The only exception from this general observation was the synthesis of the GE11-PEG$_5$-NHS ester (**11**) which is an important intermediate for the following assembly of the peptide homodimer (**6**) and homotetramer (**7**) (Scheme 2).

During the synthesis of **11** from GE11 peptide intermediate **8** with PEG$_5$-bis-NHS ester on solid support, a significant amount of peptide dimers was formed by cross-linking of two GE11 peptides being immobilized in direct vicinity to each other on the resin by the applied PEG$_5$-bis-NHS ester (Figure 4). Although low-loading resins were used during the synthesis, the distance between the peptides was so small that a substantial amount of dimers formed either using mechanical agitation or ultrasound-assisted synthesis. However, the amount of unintended cross-linking was considerably higher in the case of ultrasound-assisted synthesis as well as was the rate of NHS-ester cleavage, yielding in the GE11-PEG$_5$ acid instead of the ester: thus, the ratio between intended product **11** and undesired byproducts was shifted to the disadvantage of **11** using the ultrasound-assisted synthesis so that lower overall isolated yields of 26% were obtained using an excess of 5 equiv of PEG$_5$-bis-NHS ester. In contrast, mechanical agitation-aided conjugation gave **11** in a 46% yield by applying an excess of 8 equiv of PEG$_5$-bis-NHS ester. Other factors also affecting product yields were the solvent used (non-anhydrous DMF reduced the achievable yields due to a considerable hydrolysis of the active ester) and the cleavage time of the peptide from the resin (significantly prolonged cleavage times also caused an increased hydrolysis rate).

The homodimer and homotetramer agents **6** and **7** were obtained by first synthesizing the NODA-GA chelator-modified bis- and tetra-amines **9** and **10** (Scheme 2), which were assembled on solid support by successive conjugation of the respective HBTU or PyBOP acid-activated building block (Fmoc-Lys(Mtt)-OH, (*R*)-NODA-GA(*t*Bu)$_3$, Fmoc-NH-PEG$_3$-OH and (Fmoc-NH-Propyl)$_2$Gly-OH) followed by acidic cleavage and simultaneous deprotection, giving both products in good yields of 78% for **9** and 72% for **10**. In parallel, GE11-PEG$_5$-NHS (**11**) was completely synthesized on solid support, including the conjugation of the PEG$_5$-bis-NHS ester to peptide intermediate **8** before cleavage from the resin.

Attempts to first isolate the GE11 peptide and conjugate the PEG$_5$-bis-NHS ester in solution resulted in very low product amounts due to the formation of several side products, preventing efficient purification of the product. An alternative approach to conjugate the PEG$_5$-bis-NHS ester still on solid support to **9** and **10** to obtain the bis-NHS and tetra-NHS esters to which GE11 could have been coupled was also not successful.

Finally, the bis- and tetra-amines **9** and **10** were reacted with **11** in solution, giving the peptide homodimer **6** and the homotetramer **7** in moderate isolated yields of 23% and 20%, respectively.

https://doi.org/10.1021/acsomega.2c03407
ACS Omega 2022, 7, 27690−27702

Scheme 1. Synthesis Pathway toward the Monovalent Chelator and Linker-Modified Peptide Derivatives 1−5[a]

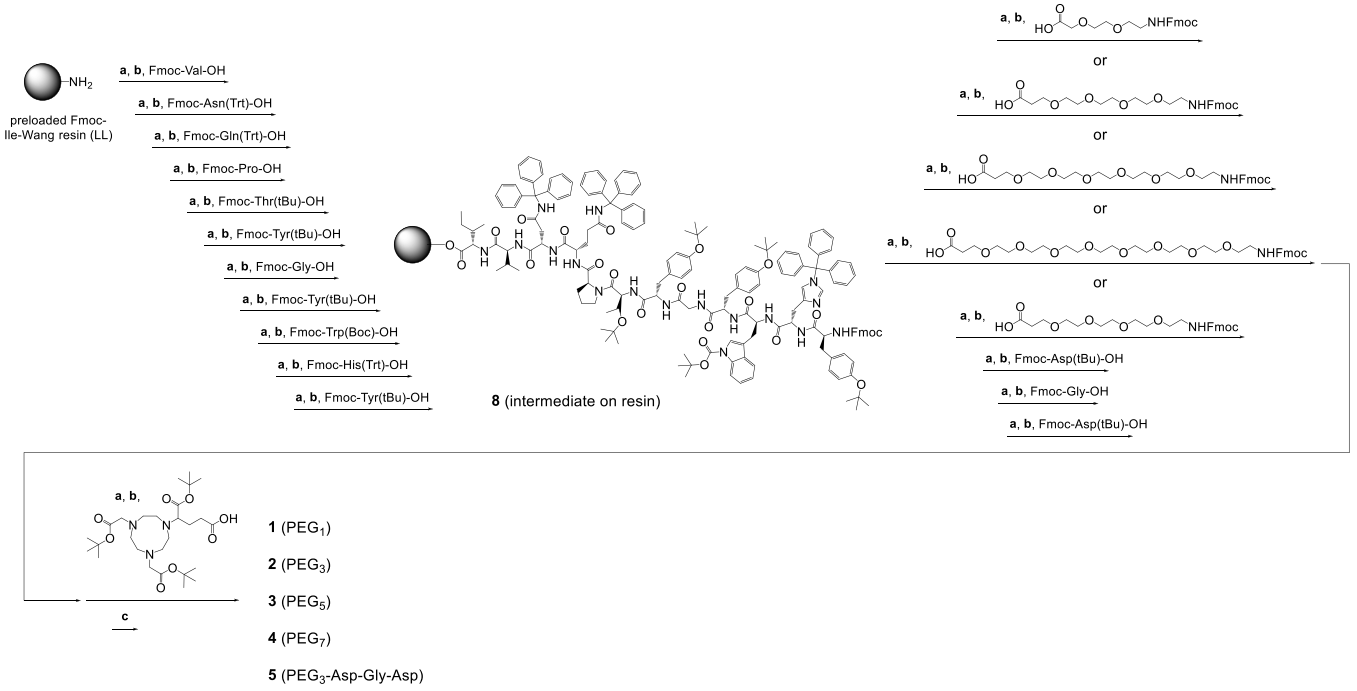

[a]Reaction conditions: (a) cleavage of Fmoc-PG: piperidine/DMF (1/1, *v*/*v*), 2 + 5 min; (b) activation of amino acids: 4.0 equiv amino acid derivative, 4.0 equiv DIPEA, 3.9 equiv HBTU in DMF, 2 min, 60 min coupling; alternatively: 2.0 equiv amino acid derivative, 2.0 equiv DIPEA, 1.9 equiv HBTU in DMF, 2 min, ultrasound-assisted coupling for 15 min; (c) cleavage of peptide from resin and simultaneous deprotection of side-chain functional groups: TFA/TIS/H_2O (95/2.5/2.5, *v*/*v*), 2−3 h.

Scheme 2. Synthesis of GE11 Peptide Dimer 6 and GE11 Tetramer 7[a]

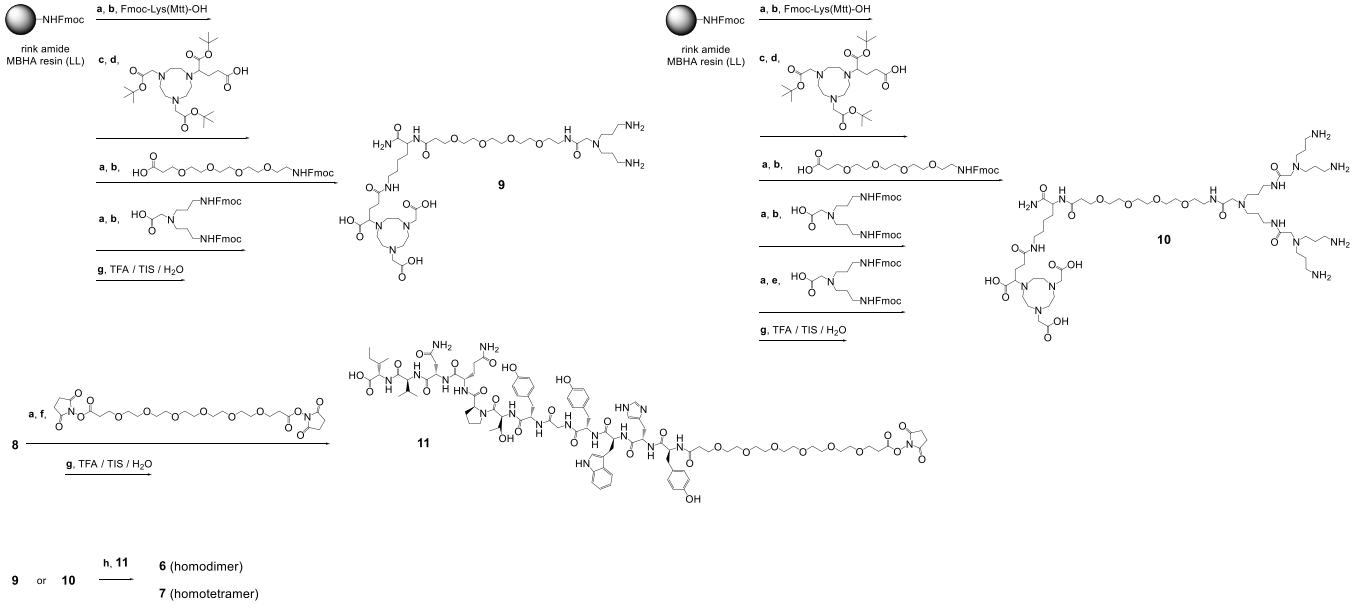

[a]Reaction conditions: (a) cleavage of Fmoc-PG: piperidine/DMF (1/1, *v*/*v*), 2 + 5 min; (b) activation of amino acids: 4.0 equiv amino acid derivative, 4.0 equiv DIPEA, 3.9 equiv HBTU in DMF, 2 min, 15 min coupling; (c) cleavage of Mtt-PG: 1% TFA in DCM, 3 × 15 min; (d) activation of (*R*)-NODA-GA(*t*Bu)$_3$: 2.0 equiv, 2.0 equiv DIPEA, 1.9 equiv PyBOP in DMF, 2 min, 30 min coupling; (e) activation of (Fmoc-NH-Propyl)$_2$Gly-OH: 6.0 equiv, 6.0 equiv DIPEA, 5.9 equiv HBTU in DMF, 2 min, 30 min coupling; (f) 8.0 equiv of PEG_5-bis-NHS ester, DMF, 1 h coupling using mechanical agitation; (g) cleavage of peptide from resin and simultaneous deprotection of side-chain functional groups: TFA/TIS/H_2O (95/2.5/2.5, *v*/*v*) for 3 h; (h) 2.6 or 4.6 equiv **11**, 6 μL DIPEA, DMF, 15 min (**6**) or 60 min (**7**) reaction.

^{68}Ga Radiolabeling of 1−7 and Evaluation of [^{68}Ga]Ga-1 to [^{68}Ga]Ga-7 in Terms of log$_{D(7.4)}$ and Stability in Human Serum. Peptide monomers **1**−**5** and multimers **6** and **7** were radiolabeled with $^{68}Ga^{3+}$ and the labeled products [^{68}Ga]Ga-**1** to [^{68}Ga]Ga-7 evaluated in terms of their hydrophilicity/lipophilicity profile and their stability toward metabolic

https://doi.org/10.1021/acsomega.2c03407
ACS Omega 2022, 7, 27690−27702

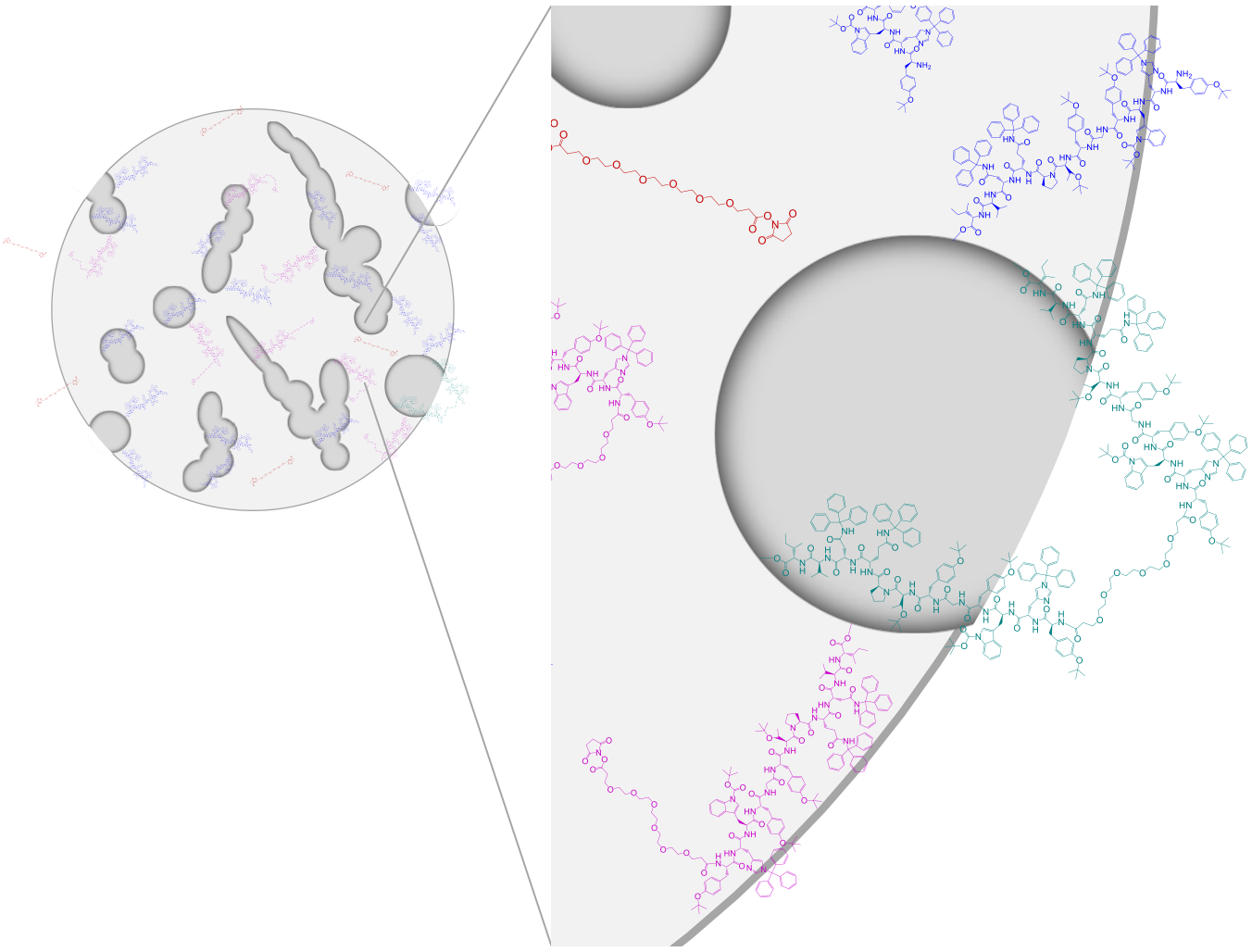

Figure 4. Schematic depiction of the cross-linking process during the synthesis of **11**: Depicted is a resin bead with bound and Fmoc-deprotected GE11 peptide intermediate **8** (blue), which is supposed to react with the PEG_5-bis-NHS ester (red); the intended conjugation product is depicted in magenta and the cross-linking product in green.

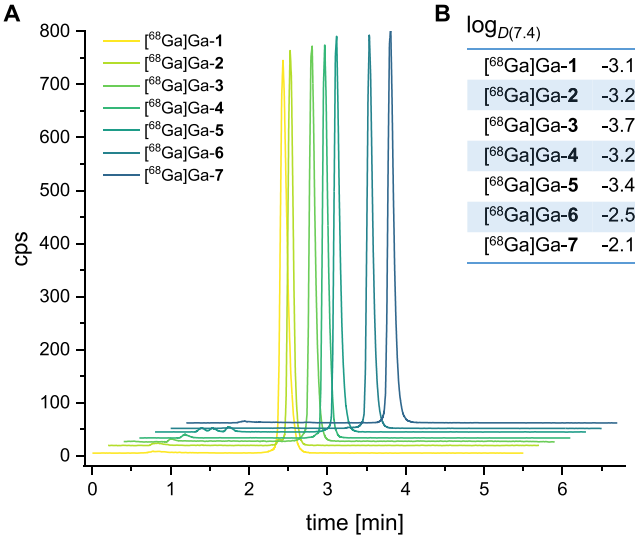

B

$log_{D(7.4)}$	
[^{68}Ga]Ga-**1**	-3.12 ± 0.06
[^{68}Ga]Ga-**2**	-3.25 ± 0.08
[^{68}Ga]Ga-**3**	-3.79 ± 0.04
[^{68}Ga]Ga-**4**	-3.28 ± 0.02
[^{68}Ga]Ga-**5**	-3.48 ± 0.21
[^{68}Ga]Ga-**6**	-2.52 ± 0.03
[^{68}Ga]Ga-**7**	-2.17 ± 0.21

C

$t_{½}$ in serum [min]	
[^{68}Ga]Ga-**1**	163.7 ± 20.3
[^{68}Ga]Ga-**2**	167.9 ± 10.5
[^{68}Ga]Ga-**3**	217.4 ± 1.0
[^{68}Ga]Ga-**4**	164.6 ± 13.4
[^{68}Ga]Ga-**5**	111.8 ± 2.4
[^{68}Ga]Ga-**6**	83.5 ± 3.7
[^{68}Ga]Ga-**7**	62.4 ± 7.1

Figure 5. (A) Analytical radio-HPLC chromatograms of [^{68}Ga]Ga-**1** to [^{68}Ga]Ga-7 obtained directly after radiolabeling, (B) $log_{D(7.4)}$ values for [^{68}Ga]Ga-**1** to [^{68}Ga]Ga-7, and(C) half-lives for [^{68}Ga]Ga-**1** to [^{68}Ga]Ga-7 in human serum.

degradation by human serum peptidases. The $^{68}Ga^{3+}$ was obtained as $^{68}GaCl_3$ by fractioned elution of a commercial $^{68}Ge/^{68}Ga$ generator system, the pH was adjusted to 3.5−4.0 by the addition of sodium acetate solution before 1−20 nmol of the

https://doi.org/10.1021/acsomega.2c03407
ACS Omega 2022, 7, 27690−27702

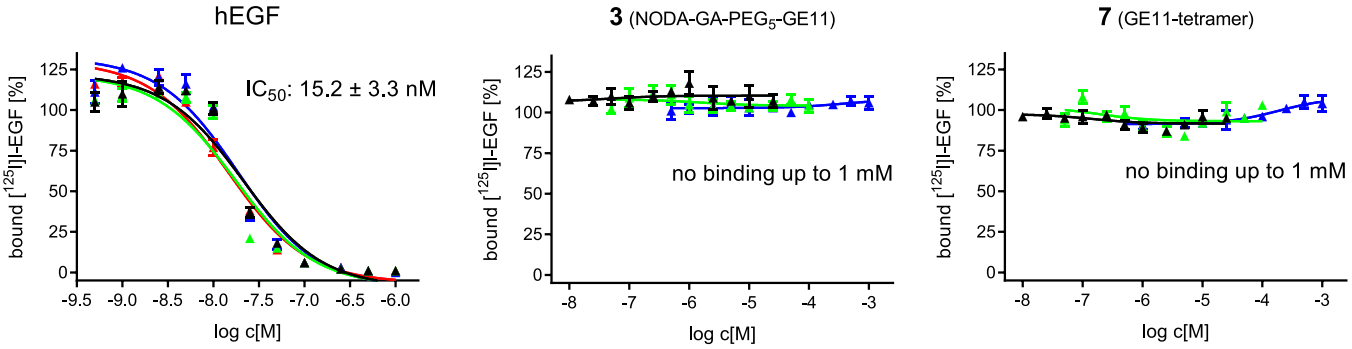

Figure 6. Graphical depiction of the results of the competitive displacements assays of hEGF, **3**, and **7** on EGFR-positive A431 cells using [^{125}I]I-EGF as the competitor.

respective precursor **1**−**7** were added, and the labeling reaction was carried out. Using NODA-GA as chelating agents instead of the more common DOTA ((1,4,7,10-tetraazacyclododecane-1,4,7,10-tetrayl)tetraacetic acid) allows labeling at much milder temperatures (45 °C instead of 90−100 °C) within short reaction times of 10 min, giving stable complexes.[20] The labeled agents [^{68}Ga]Ga-**1** to [^{68}Ga]Ga-**7** were obtained in radiochemical yields and purities of ≥97% (Figure 5A) as well as non-optimized molar activities of 41−104 GBq/μmol, starting from 230 to 310 MBq $^{68}Ga^{3+}$.

[^{68}Ga]Ga-**1** to [^{68}Ga]Ga-**7** were evaluated in terms of their hydrophilicity/lipophilicity profiles as this is a good indicator for the likely major route of excretion during an *in vivo* application of the radiotracer.[35,36] The $\log_{D(7.4)}$ values were determined by distribution experiments and partition of the respective radiotracer between an aqueous phosphate buffer phase at pH 7.4 and 1-octanol. The results of these evaluations (Figure 5B) showed high hydrophilicity of the monovalent radioligands [^{68}Ga]Ga-**1** to [^{68}Ga]Ga-**5** of −3.12 ± 0.06 to −3.79 ± 0.04, whereas the peptide dimer [^{68}Ga]Ga-**6** and tetramer [^{68}Ga]Ga-**7** showed considerably lower hydrophilicities of −2.52 ± 0.03 and −2.17 ± 0.21, respectively, nevertheless pointing to a presumably mainly renal clearance of all agents. High hydrophilicity of the radiotracers is beneficial for their application in PET imaging as EGFR-specific peptidic radiotracers are interesting agents for the visualization of several different malignancies (vide supra), but among these especially, the delineation of hepatocellular carcinomas (HCCs) and liver metastases of colon carcinomas would be an important application as these express the EGFR to a high extent and are usually difficult to detect using common radiotracers.[37,38] A high unspecific uptake of the radiopeptides into the liver would impede lesion detection and delineation especially in these two malignancies, making high hydrophilicity of the radiopeptides mandatory for successful tumor imaging.

Another important factor influencing the applicability of a radiotracer is its stability. Thus, the stability of [^{68}Ga]Ga-**1** to [^{68}Ga]Ga-**7** was evaluated by incubating them in human serum as a standard *in vitro* stability test, showing the stability toward degradation by human serum peptidases. For this purpose, the respective radiolabeled agent was incubated in commercially available pooled human serum of healthy donors at 37 °C and aliquots of the mixtures were analyzed after defined time points of 0, 5, 15, 30, 45, 60, and 90 min by analytical radio-HPLC in order to determine the intact fraction of the radiopeptides. From these data (Figure 5C and Figure S11−S17), the serum half-life of each radioligand was determined, showing values between 112 and 217 min for the peptide monomers [^{68}Ga]Ga-**1** to [^{68}Ga]Ga-**5** and 84 and 62 min for the peptide dimer [^{68}Ga]Ga-**6** and tetramer [^{68}Ga]Ga-**7**, respectively. Within the line of the peptide monomers [^{68}Ga]Ga-**1** to [^{68}Ga]Ga-**4**, the length of the introduced PEG linker does not seem to have a significant influence on the peptide stability, whereas the introduction of the additional amino acid sequence Asp-Gly-Asp seems to introduce another point of attack for peptidases: the half-life of [^{68}Ga]Ga-**5** is considerably decreased by half compared to its analogue [^{68}Ga]Ga-**3**, being composed of the same structure elements (GE11 peptide, PEG_3-linker, NODA-GA chelator) apart from the Asp-Gly-Asp motive. For the peptide multimers [^{68}Ga]Ga-**6** and [^{68}Ga]Ga-**7**, considerably shorter half-lives were interestingly observed compared to the monomers. However, it has also been shown that, despite degradation of peptide copies within a peptide multimer, the remaining intact peptide units nevertheless enable us to still take advantage of the favorable properties of peptide multimers such as increased avidity, prolonged bioavailability, and increased probability of target binding and rebinding.[39] Overall, the half-lives of all radiopeptides are thus in a reasonable range for PET imaging using the clinically most relevant diagnostic radiometal ^{68}Ga.

***In Vitro* Tumor Cell Uptake Studies of [^{68}Ga]Ga-1 to [^{68}Ga]Ga-7 and Competitive Displacement Assays on A431 Cells.** Finally, we determined if the developed radioligands still show the ability to target EGFR-expressing tumor cells.

First, we performed cell uptake studies[40] on A431 cells (human epidermoid carcinoma cell line), which are known to highly express the EGFR[41] and are thus the standard cell line for the evaluation of EGFR-specific radioligands.[42,43] For this purpose, we incubated the cells in the presence and absence of the endogenous EGFR ligand hEGF (human epidermal growth factor) with the respective ^{68}Ga-labeled peptide and quantified EGFR-specific and EGFR-unspecific cell interactions differentiated by membrane-bound and internalized activity after 30 min, 1, 2, and 3 h. However, we were not able to detect a measurable EGFR-specific uptake into the cells but only a relatively high unspecific interaction of the tracers with the cells. This finding is in line with former reports, mentioning a high unspecific interaction of GE11-based radioligands with tumor cell lines of different origin.[13,17] These results seem to indicate that the proposed aggregation of the radiopeptides and the resulting limited receptor interaction probability discussed above should not be the reason for the absent tumor cell uptake of GE11-based tracers into EGFR-positive cells as the chosen hydrophilic molecular designs, especially in the case of the twice negatively charged derivative [^{68}Ga]Ga-**5**, should hinder aggregation. Also, the introduction of PEG linkers of different

https://doi.org/10.1021/acsomega.2c03407
ACS Omega 2022, 7, 27690−27702

lengths was not able to result in an EGFR-specific cell uptake of the radioligands being facilitated by an increased hydrophilicity and a larger distance between the GE11 peptide and the chelator/^{68}Ga complex. Thus, at least some difference in tumor cell uptake behavior should have been observed between the different radiotracers if a hydrophobicity-driven aggregation were the main reason for the absent EGFR-specific tumor cell interaction.

In contrast, a previous work on phthalocyanine (Pc) conjugates of GE11 showed that the introduction of a hydrophobic structure element at the *N*-terminus of the peptide can even result in a positive contribution to receptor binding. It was found that phthalocyanines, especially when being attached to the peptide at an appropriate distance, can support EGF receptor binding by Pc-induced anchoring near the hydrophobic region around amino acid residues Tyr89, Tyr93, and Phe148 outside the EGFR binding pocket.[44]

Due to the absent EGFR-mediated tumor cell uptake of [^{68}Ga]Ga-**1** to [^{68}Ga]Ga-**7**, we further evaluated **1**−**7** and also unmodified GE11 for their ability to displace hEGF from its receptor and thus with respect to their *in vitro* receptor affinity profile on the same cell line. By this, we intended to determine potential positive effects of introduced hydrophilic structure elements or multivalency on EGFR-specific binding. For this purpose, we conducted competitive displacement assays using [^{125}I]I-EGF as the competitor and endogenous hEGF as internal reference standard with known high affinity for this receptor type.[18] The results of these assays are depicted in Figure 6 (exemplary binding curves obtained for hEGF, **3**, and **7**) and Figures S18−S23 (binding curves for the rest of the agents, namely, **1**, **2**, **4**−**6**, and unmodified GE11), showing a high EGFR affinity of hEGF with an IC_{50} value of 15.2 ± 3.3 nM but no measurable affinity of the newly developed monovalent or multivalent agents up to a concentration of 1 mM.

These results match those of the internalization assays and are also in accordance to several examples in the literature where a rather heterogeneous picture is drawn with regard to binding affinities of GE11-based compounds to the EGFR: While many studies did not show/investigate EGFR affinities at all,[5] there are certainly examples of GE11-based compounds showing good affinities to this receptor type.[13,14] However, the bigger part of publications dealing with the development of GE11-based compounds describe effects similar to those observed here, namely, that no or very low affinities to the EGFR were found.[10,11,17,18] This heterogeneous literature situation is mostly justified by the fact that GE11 presumably shows a relevant EGFR affinity only in a multivalent form, as for example, during its discovery by phage display[9] or in the case of GE11-modified dendrimers, polymers, or particle-based systems.[45−48] This is confirmed by a recent study that addressed this very question and found an unmeasurably low affinity for the unmodified GE11 monomer of more than 1 mM on different EGFR-positive cell lines (among these, A431, MDA-MB-468, and U87MG cells), while showing a moderate affinity for a GE11 polymer (GE11-modified polyethyleneimine-polyethyleneglycol) of 1900 ± 432 nM.[18] This affinity profile is however still considerably worse than the affinity of hEGF to the EGFR of 5.1 ± 0.9 nM being determined in the same study.

This clearly demonstrates the effect of insufficient affinity of GE11 monomers and is confirmed by the results of the present study. However, the GE11-based agents of higher valency (dimer and tetramer) developed here were also not able to produce agents of measurable affinities, so it can be assumed that GE11 indeed shows relevant affinity to the EGFR only for considerably higher peptide copy numbers per molecule. The development of GE11-based polymers however remains a challenge and matching a defined molecular structure is difficult to achieve, which is nevertheless highly desirable for the clinical application of a receptor-specific agent.

To develop monovalent GE11 peptide-based radiotracers or analogues carrying a low number of GE11 peptide units does thus not seem to be a promising approach in order to achieve a considerable EGFR-specific tumor uptake and as a result a relevant tumor visualization specificity and sensitivity.

CONCLUSIONS

We were able to show in the present study that the points having been discussed to be potential reasons for the suboptimal pharmacokinetic properties of the GE11-based radiopeptides developed for *in vivo* tumor imaging so far are in part correct. One potential problem previously identified is a hydrophobicity-induced aggregation of the peptide, which could be the reason for a lacking EGF receptor interaction of the peptidic lead structure. The results of our work however suggest that this appears to be only a small part of the problem, if any, as we developed several rather hydrophilic radiolabeled GE11 derivatives, one of which further carrying mutually repulsive charged functional groups with all of them showing no EGF receptor targeting ability. The other potential problem previously identified is a rather low affinity of the isolated GE11 lead structure and the necessity to incorporate a high number of peptide copies into a polymer matrix to achieve sufficient affinities of the constructs. Our results support this theory and show that even GE11-based multimers of low valency (dimer and tetramer) are still too small to enable a sufficient target receptor interaction.

In conclusion, a monovalent GE11 peptide or a low number of GE11 peptide units per radiotracer molecule appears to be of limited utility to achieve a relevant EGFR interaction, impeding the development of non-protein-based EGFR-specific radioligands for tumor diagnosis and therapy based on this peptide lead.

ASSOCIATED CONTENT

Supporting Information

The Supporting Information is available free of charge at https://pubs.acs.org/doi/10.1021/acsomega.2c03407.

HR-ESI-MS spectra of **1**−**7** and **9**−**11**, results of the stability tests of [^{68}Ga]Ga-**1** to [^{68}Ga]Ga-**7** in human serum, and graphical depiction of the results of the competitive displacements assays of **1**, **2**, **4**−**6** and unmodified GE11 on EGFR-positive A431 cells (PDF)

AUTHOR INFORMATION

Corresponding Author

Carmen Wängler − *Biomedical Chemistry, Clinic of Radiology and Nuclear Medicine, Medical Faculty Mannheim, Heidelberg University, 68167 Mannheim, Germany;* orcid.org/0000-0003-1161-8669; Email: Carmen.Waengler@medma.uni-heidelberg.de

Authors

Benedikt Judmann − *Biomedical Chemistry, Clinic of Radiology and Nuclear Medicine, Medical Faculty Mannheim, Heidelberg University, 68167 Mannheim, Germany;*

https://doi.org/10.1021/acsomega.2c03407
ACS Omega 2022, 7, 27690−27702

Molecular Imaging and Radiochemistry, Clinic of Radiology and Nuclear Medicine, Medical Faculty Mannheim, Heidelberg University, 68167 Mannheim, Germany

Diana Braun − *Biomedical Chemistry, Clinic of Radiology and Nuclear Medicine, Medical Faculty Mannheim, Heidelberg University, 68167 Mannheim, Germany; Molecular Imaging and Radiochemistry, Clinic of Radiology and Nuclear Medicine, Medical Faculty Mannheim, Heidelberg University, 68167 Mannheim, Germany*

Ralf Schirrmacher − *Department of Oncology, Division of Oncological Imaging, University of Alberta, T6G 1Z2 Edmonton, AB, Canada;* orcid.org/0000-0002-7098-3036

Björn Wängler − *Molecular Imaging and Radiochemistry, Clinic of Radiology and Nuclear Medicine, Medical Faculty Mannheim, Heidelberg University, 68167 Mannheim, Germany*

Gert Fricker − *Institute of Pharmacy and Molecular Biotechnology, University of Heidelberg, 69120 Heidelberg, Germany;* orcid.org/0000-0003-3894-961X

Complete contact information is available at: https://pubs.acs.org/10.1021/acsomega.2c03407

Author Contributions

⊥B.J. and D.B. contributed equally to this work.

Funding

This research project is part of the Forschungscampus M²OLIE and funded by the German Federal Ministry of Education and Research (BMBF) within the Framework "Research Campus—Public−Private Partnership for Innovation" under the funding codes 13GW0389B and 13GW0388A.

Notes

The authors declare no competing financial interest.

■ ACKNOWLEDGMENTS

The authors thank Dr. Werner Spahl (LMU Munich) for performing the HR-ESI mass spectroscopy and Tobias Timmermann (RKU Heidelberg) for performing the NMR experiments.

■ REFERENCES

(1) Kaufman, N. E. M.; Dhingra, S.; Jois, S. D.; Vicente, M. D. H. Molecular Targeting of Epidermal Growth Factor Receptor (EGFR) and Vascular Endothelial Growth Factor Receptor (VEGFR). *Molecules* **2021**, *26*, 1076.

(2) Wee, P.; Wang, Z. X. Epidermal Growth Factor Receptor Cell Proliferation Signaling Pathways. *Cancers* **2017**, *9*, 52.

(3) Sigismund, S.; Avanzato, D.; Lanzetti, L. Emerging functions of the EGFR in cancer. *Mol. Oncol.* **2018**, *12*, 3−20.

(4) Rinne, S. S.; Orlova, A.; Tolmachev, V. PET and SPECT Imaging of the EGFR Family (RTK Class I) in Oncology. *Int. J. Mol. Sci.* **2021**, *22*, 3663.

(5) Genta, I.; Chiesa, E.; Colzani, B.; Modena, T.; Conti, B.; Dorati, R. GE11 Peptide as an Active Targeting Agent in Antitumor Therapy: A Minireview. *Pharmaceutics* **2018**, *10*, 2.

(6) Thomas, R.; Zhang, W. H. Rethink of EGFR in Cancer With Its Kinase Independent Function on Board. *Front. Oncol.* **2019**, *9*, 800.

(7) Santarius, T.; Shipley, J.; Brewer, D.; Stratton, M. R.; Cooper, C. S. A census of amplified and overexpressed human cancer genes. *Nat. Rev. Cancer* **2010**, *10*, 59−64.

(8) Yarden, Y.; Pines, G. The ERBB network: at last, cancer therapy meets systems biology. *Nat. Rev. Cancer* **2012**, *12*, 553−563.

(9) Li, Z. H.; Zhao, R. J.; Wu, X. H.; Sun, Y.; Yao, M.; Li, J. J.; Xu, Y. H.; Gu, J. R. Identification and characterization of a novel peptide ligand of epidermal growth factor receptor for targeted delivery of therapeutics. *FASEB J.* **2005**, *19*, 1978−1985.

(10) Rahmanian, N.; Hosseinimehr, S. J.; Khalaj, A.; Noaparast, Z.; Abedi, S. M.; Sabzevari, O. 99mTc-radiolabeled GE11-modified peptide for ovarian tumor targeting. *Daru* **2017**, *25*, 13.

(11) Rahmanian, N.; Hosseinimehr, S. J.; Khalaj, A.; Noaparast, Z.; Abedi, S. M.; Sabzevari, O. 99mTc labeled HYNIC-EDDA/tricine-GE11 peptide as a successful tumor targeting agent. *Med. Chem. Res.* **2018**, *27*, 890−902.

(12) Dissoki, S.; Hagooly, A.; Elmachily, S.; Mishani, E. Labeling approaches for the GE11 peptide, an epidermal growth factor receptor biomarker. *J. Labelled Compd. Radiopharm.* **2011**, *54*, 693−701.

(13) Jiao, H. L.; Zhao, X. M.; Han, J. Y.; Zhang, J. M.; Wang, J. F. Synthesis of a novel 99mTc labeled GE11 peptide for EGFR SPECT imaging. *Int. J. Radiat. Biol.* **2020**, *96*, 1443−1451.

(14) Li, X. L.; Hu, K. Z.; Liu, W. F.; Wei, Y. F.; Sha, R. H.; Long, Y. X.; Han, Y. J.; Sun, P. H.; Wu, H. B.; Li, G. P.; Tang, G. H.; Huang, S. Synthesis and evaluation of [18F]FP-Lys-GE11 as a new radiolabeled peptide probe for epidermal growth factor receptor (EGFR) imaging. *Nucl. Med. Biol.* **2020**, *90-91*, 84−92.

(15) Yu, H. M.; Chen, J. H.; Lin, K. L.; Lin, W. J. Synthesis of 68Ga-labeled NOTA-RGD-GE11 heterodimeric peptide for dual integrin and epidermal growth factor receptor-targeted tumor imaging. *J. Labelled Compd. Radiopharm.* **2015**, *58*, 299−303.

(16) Chen, C. J.; Chan, C. H.; Lin, K. L.; Chen, J. H.; Tseng, C. H.; Wang, P. Y.; Chien, C. Y.; Yu, H. M.; Lin, W. J. 68Ga-labelled NOTA-RGD-GE11 peptide for dual integrin and EGFR-targeted tumour imaging. *Nucl. Med. Biol.* **2019**, *68-69*, 22−30.

(17) Striese, F.; Sihver, W.; Gao, F.; Bergmann, R.; Walther, M.; Pietzsch, J.; Steinbach, J.; Pietzsch, H. J. Exploring pitfalls of 64Cu-labeled EGFR-targeting peptide GE11 as a potential PET tracer. *Amino Acids* **2018**, *50*, 1415−1431.

(18) Abourbeh, G.; Shir, A.; Mishani, E.; Ogris, M.; Rodl, W.; Wagner, E.; Levitzki, A. PolyIC GE11 polyplex inhibits EGFR-overexpressing tumors. *IUBMB Life* **2012**, *64*, 324−330.

(19) Wellings, D. A.; Atherton, E. Standard Fmoc protocols. *Methods Enzymol.* **1997**, *289*, 44−67.

(20) Wängler, C.; Wängler, B.; Lehner, S.; Elsner, A.; Todica, A.; Bartenstein, P.; Hacker, M.; Schirrmacher, R. A Universally Applicable 68Ga-Labeling Technique for Proteins. *J. Nucl. Med.* **2011**, *52*, 586−591.

(21) Litau, S.; Seibold, U.; Vall-Sagarra, A.; Fricker, G.; Wangler, B.; Wangler, C. Comparative Assessment of Complex Stabilities of Radiocopper Chelating Agents by a Combination of Complex Challenge and in vivo Experiments. *ChemMedChem* **2015**, *10*, 1200−1208.

(22) Däpp, S.; Garayoa, E. G.; Maes, V.; Brans, L.; Tourwe, D. A.; Muller, C.; Schibli, R. PEGylation of Tc-99m-labeled bombesin analogues improves their pharmacokinetic properties. *Nucl. Med. Biol.* **2011**, *38*, 997−1009.

(23) Hausner, S. H.; Bauer, N.; Hu, L. N. Y.; Knight, L. M.; Sutcliffe, J. L. The Effect of Bi-Terminal PEGylation of an Integrin alpha(v)-beta(6)-Targeted F-18 Peptide on Pharmacokinetics and Tumor Uptake. *J. Nucl. Med.* **2015**, *56*, 784−790.

(24) Antunes, P.; Ginj, M.; Walter, M. A.; Chen, J. H.; Reubi, J. C.; Maecke, H. R. Influence of different spacers on the biological profile of a DOTA-somatostatin analogue. *Bioconjugate Chem.* **2007**, *18*, 84−92.

(25) Niedermoser, S.; Chin, J.; Wängler, C.; Kostikov, A.; Bernard-Gauthier, V.; Vogler, N.; Soucy, J. P.; McEwan, A. J.; Schirrmacher, R.; Wängler, B. In Vivo Evaluation of F-18-SiFAlin-Modified TATE: A Potential Challenge for Ga-68-DOTATATE, the Clinical Gold Standard for Somatostatin Receptor Imaging with PET. *J. Nucl. Med.* **2015**, *56*, 1100−1105.

(26) Summer, D.; Rangger, C.; Klingler, M.; Laverman, P.; Franssen, G. M.; Lechner, B. E.; Orasch, T.; Haas, H.; von Guggenberg, E.; Decristoforo, C. Exploiting the Concept of Multivalency with Ga-68- and Zr-89-Labelled Fusarinine C-Minigastrin Bioconjugates for Targeting CCK2R Expression. *Contrast Media Mol. Imaging* **2018**, *78*, 3171794.

(27) Wu, Y.; Zhang, X. Z.; Xiong, Z. M.; Cheng, Z.; Fisher, D. R.; Liu, S.; Gambhir, S. S.; Chen, X. Y. MicroPET imaging of glioma integrin alpha(V)beta(3) expression using Cu-64-labeled tetrameric RGD peptide. *J. Nucl. Med.* **2005**, *46*, 1707−1718.
(28) Dijkgraaf, I.; Yim, C. B.; Franssen, G. M.; Schuit, R. C.; Luurtsema, G.; Liu, S. A.; Oyen, W. J. G.; Boerman, O. C. PET imaging of alpha(v)beta(3) integrin expression in tumours with Ga-68-labelled mono-, di- and tetrameric RGD peptides. *Eur. J. Nucl. Med. Mol. Imaging* **2011**, *38*, 128−137.
(29) Liu, S. Radiolabeled Cyclic RGD Peptides as Integrin alpha(v)beta(3)-Targeted Radiotracers: Maximizing Binding Affinity via Bivalency. *Bioconjugate Chem.* **2009**, *20*, 2199−2213.
(30) Vauquelin, G.; Charlton, S. J. Exploring avidity: understanding the potential gains in functional affinity and target residence time of bivalent and heterobivalent ligands. *Brit. J. Pharmacol.* **2013**, *168*, 1771−1785.
(31) Pedersen, S. L.; Tofteng, A. P.; Malik, L.; Jensen, K. J. Microwave heating in solid-phase peptide synthesis. *Chem. Soc. Rev.* **2012**, *41*, 1826−1844.
(32) Raheem, S. J.; Schmidt, B. W.; Solomon, V. R.; Salih, A. K.; Price, E. W. Ultrasonic-Assisted Solid-Phase Peptide Synthesis of DOTA-TATE and DOTA-linker-TATE Derivatives as a Simple and Low-Cost Method for the Facile Synthesis of Chelator-Peptide Conjugates. *Bioconjugate Chem.* **2021**, *32*, 1204−1213.
(33) Merlino, F.; Tomassi, S.; Yousif, A. M.; Messere, A.; Marinelli, L.; Grieco, P.; Novellino, E.; Cosconati, S.; Di Maro, S. Boosting Fmoc Solid-Phase Peptide Synthesis by Ultrasonication. *Org. Lett.* **2019**, *21*, 6378−6382.
(34) Wolczanski, G.; Plociennik, H.; Lisowski, M.; Stefanowicz, P. A faster solid phase peptide synthesis method using ultrasonic agitation. *Tetrahedron Lett.* **2019**, *60*, 1814−1818.
(35) Garayoa, E. G.; Schweinsberg, C.; Maes, V.; Brans, L.; Blauenstein, P.; Tourwe, D. A.; Schibli, R.; Schubiger, P. A. Influence of the Molecular Charge on the Biodistribution of Bombesin Analogues Labeled with the [Tc-99m(CO)(3)]-Core. *Bioconjugate Chem.* **2008**, *19*, 2409−2416.
(36) Glaser, M.; Morrison, M.; Solbakken, M.; Arukwe, J.; Karlsen, H.; Wiggen, U.; Champion, S.; Kindberg, G. M.; Cuthbertson, A. Radiosynthesis and biodistribution of cyclic RGD peptides conjugated with novel [18F]fluorinated aldehyde-containing prosthetic groups. *Bioconjugate Chem.* **2008**, *19*, 951−957.
(37) Choi, K. J.; Baik, I. H.; Ye, S. K.; Lee, Y. H. Molecular Targeted Therapy for Hepatocellular Carcinoma: Present Status and Future Directions. *Biol. Pharm. Bull.* **2015**, *38*, 986−991.
(38) Feng, Q. Y.; Wei, Y.; Chen, J. W.; Chang, W. J.; Ye, L. C.; Zhu, D. X.; Xu, J. M. Anti-EGFR and anti-VEGF agents: Important targeted therapies of colorectal liver metastases. *World J. Gastroenterol.* **2014**, *20*, 4263−4275.
(39) Summer, D.; Kroess, A.; Woerndle, R.; Rangger, C.; Klingler, M.; Haas, H.; Kremser, L.; Lindner, H. H.; von Guggenberg, E.; Decristoforo, C. Multimerization results in formation of re-bindable metabolites: A proof of concept study with FSC-based minigastrin imaging probes targeting CCK2R expression. *PLoS One* **2018**, *13*, No. e0201224.
(40) Summer, D.; Grossrubatscher, L.; Petrik, M.; Michalcikova, T.; Novy, Z.; Rangger, C.; Klingler, M.; Haas, H.; Kaeopookum, P.; von Guggenberg, E.; Haubner, R.; Decristoforo, C. Developing Targeted Hybrid Imaging Probes by Chelator Scaffolding. *Bioconjugate Chem.* **2017**, *28*, 1722−1733.
(41) Benedetto, S.; Pulito, R.; Crich, S. G.; Tarone, G.; Aime, S.; Silengo, L.; Hamm, J. Quantification of the expression level of integrin receptor alpha(V)beta(3) in cell lines and MR imaging with antibody-coated iron oxide particles. *Magn. Reson. Med.* **2006**, *56*, 711−716.
(42) Oroujeni, M.; Xu, T. Q.; Gagnon, K.; Rinne, S. S.; Weis, J.; Garousi, J.; Andersson, K. G.; Lofblom, J.; Orlova, A.; Tolmachev, V. The Use of a Non-Conventional Long-Lived Gallium Radioisotope Ga-66 Improves Imaging Contrast of EGFR Expression in Malignant Tumours Using DFO-ZEGFR:2377 Affibody Molecule. *Pharmaceutics* **2021**, *13*, 292.
(43) Chang, A. J.; De Silva, R. A.; Lapi, S. E. Development and Characterization of Zr-89-Labeled Panitumumab for Immuno-Positron Emission Tomographic Imaging of the Epidermal Growth Factor Receptor. *Mol. Imaging* **2013**, *12*, 17−27.
(44) Ongarora, B. G.; Fontenot, K. R.; Hu, X. K.; Sehgal, I.; Satyanarayana-Jois, S. D.; Vicente, D. G. H. Phthalocyanine-Peptide Conjugates for Epidermal Growth Factor Receptor Targeting. *J. Med. Chem.* **2012**, *55*, 3725−3738.
(45) Grünwald, G. K.; Vetter, A.; Klutz, K.; Willhauck, M. J.; Schwenk, N.; Senekowitsch-Schmidtke, R.; Schwaiger, M.; Zach, C.; Wagner, E.; Goke, B.; Holm, P. S.; Ogris, M.; Spitzweg, C. EGFR-Targeted Adenovirus Dendrimer Coating for Improved Systemic Delivery of the Theranostic NIS Gene. *Mol. Ther.–Nucleic Acids* **2013**, *2*, No. e131.
(46) Klutz, K.; Schaffert, D.; Willhauck, M. J.; Grünwald, G. K.; Haase, R.; Wunderlich, N.; Zach, C.; Gildehaus, F. J.; Senekowitsch-Schmidtke, R.; Goke, B.; Wagner, E.; Ogris, M.; Spitzweg, C. Epidermal Growth Factor Receptor-targeted I-131-therapy of Liver Cancer Following Systemic Delivery of the Sodium Iodide Symporter Gene. *Mol. Ther.* **2011**, *19*, 676−685.
(47) Mickler, F. M.; Mockl, L.; Ruthardt, N.; Ogris, M.; Wagner, E.; Brauchle, C. Tuning Nanoparticle Uptake: Live-Cell Imaging Reveals Two Distinct Endocytosis Mechanisms Mediated by Natural and Artificial EGFR Targeting Ligand. *Nano Lett.* **2012**, *12*, 3417−3423.
(48) Song, S. X.; Liu, D.; Peng, J. L.; Sun, Y.; Li, Z. H.; Gu, J. R.; Xu, Y. H. Peptide ligand-mediated liposome distribution and targeting to EGFR expressing tumor in vivo. *Int. J. Pharm.* **2008**, *363*, 155−161.

https://doi.org/10.1021/acsomega.2c03407
ACS Omega 2022, 7, 27690−27702